香港天文台
HONG KONG OBSERVATORY

Reprint 554

Prototype Automatic LIDAR-based Wind Shear Detection Algorithms

B.L. Choy, O.S.M. Lee, C.M. Shun & C.M. Cheng

11th Conference on Aviation, Range, and Aerospace Meteorology,

American Meteorological Society,

Hyannis, MA, USA, 4-8 October 2004

P4.11 PROTOTYPE AUTOMATIC LIDAR-BASED WIND SHEAR DETECTION ALGORITHMS

B.L. Choy*, Olivia S.M. Lee, C.M. Shun, C.M. Cheng
Hong Kong Observatory, Hong Kong, China

1. INTRODUCTION

The Hong Kong International Airport (HKIA) at Chek Lap Kok (CLK) came into operation on 6 July 1998. It has two parallel northeast-southwest oriented runways designated as RWY 07L/25R and RWY 07R/25L. The airport is situated to the north of Lantau Island which is quite mountainous. Figure 1 illustrates the complex terrain of Lantau Island and the location of HKIA.

Since airport opening, a Terminal Doppler Weather Radar (TDWR) has been used to detect and warn low-level wind shear. While the TDWR has proved to be effective in rainy weather, reports received from aircraft pilots landing at or taking off from the airport indicate that low-level wind shear also occurs under clear-air conditions. To overcome this shortcoming, a Doppler LIght Detection And Ranging (LIDAR) System was installed in mid-2002 to monitor wind flow around the airport. The LIDAR is the first of its kind in the world for operational airport weather alerting. Shun and Lau (2002) provided a detailed description of the LIDAR and the considerations in its implementation. Interesting LIDAR observations of terrain-induced phenomena downwind of Lantau were documented by Shun et al (2003) and Shun et al (2004).

Since its installation, the LIDAR has been used by aviation forecasters of the Hong Kong Observatory (HKO) for issuing wind shear alerts to aircraft. To further improve the timeliness of the alerts, on-going efforts are being undertaken to develop LIDAR-based automatic wind shear detection algorithms. This paper presents the development of these algorithms. LIDAR scan strategy and computation methods will be discussed. Initial evaluation of the performance of the algorithms will also be presented.

* Corresponding author address: B.L. Choy, Hong Kong Observatory, 134A Nathan Road, Hong Kong, China; e-mail: blchoy@hko.gov.hk

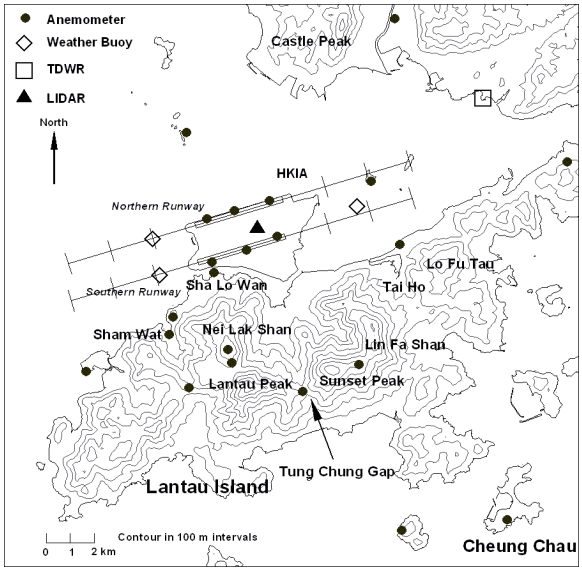

Figure 1. Map of HKIA, its approach/departure corridors and surrounding areas. Terrain contours are given in 100 m intervals.

2. LIDAR LOCATION AND SCAN STRATEGY

The LIDAR is located on the roof-top of the Air Traffic Control Complex (ATCX) between the two runways (see Figure 1). At an altitude of about 50 m above MSL, or about 43 m above the runways, the LIDAR scanner has unobstructed view towards all directions apart from the northwest sector where the Air Traffic Control Tower (ATCT) is located.

With a location slightly east of the centre of the airport and a horizontal range of around 8.5 km, the LIDAR provides Doppler wind data out to about 3 NM (or 5.6 km) from the runway ends to the west and out to about 4 NM (or 7.4 km) to the east.

As regards laser safety, the LIDAR is classified as Class 1M, i.e. the laser equipment is safe under reasonably foreseeable conditions of operation, but may be hazardous if the user employs optics within the beam (IEC, 2001). To enhance laser safety to personnel at the ATCT to the northwest and residential buildings to the southeast of the LIDAR site, sector

blanking is implemented to prevent laser transmission in these sectors.

To monitor wind shear over the approach/departure corridors (typically at 3 and 6 degrees elevation from the horizontal plane respectively), the initial LIDAR scan strategy included azimuthal scans (or Plan Position Indicator (PPI) scans) at 0.0, 1.0 and 4.5 degrees as well as a number of Range Height Indicator (RHI) scans towards the runway corridors until recently (see Section 4.3). The range resolution in the radial direction is 100 m. The high pulse repetition frequency (PRF) of 500 Hz of the transceiver allows sampling at 10 radials (or line of sight (LOS)) per second. This sampling rate enables a revisit time of a couple of minutes in scanning around the airport for collecting Doppler wind data for wind shear monitoring by forecasters as well as development of automatic wind shear detection algorithms.

3. ALGORITHM I: RADIAL SHEAR ALERT GENERATION ALGORITHM

3.1 Description of Algorithm

Located near the centre of the airport, the LIDAR beams and the flight paths intersect at angles of less than 30 degrees. With such reasonable alignment with the flight paths, radial shear of Doppler velocities along the radials of the PPI scans could be computed to estimate the wind shear along the flight paths (see Figure 2(a)).

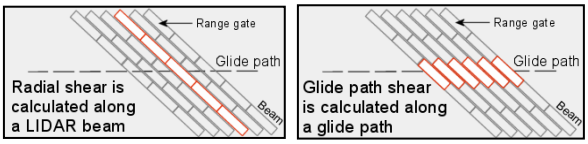

Figures 2(a) (Left) and 2(b) (Right). Illustrations showing how radial shear and glide path shear are calculated respectively.

Formulated in a framework similar to that of the TDWR Microburst and Gust Front Detection Algorithm (Merritt et al, 1989), for each PPI scan, the Radial shear Alert Generation Algorithm (RAGA) first identifies shear segments on each radial beam according to a predefined shear threshold. Adjacent shear segments within the same scan are then clustered together to form shear features. If a total shear with Doppler radial velocity difference greater than or equal to 15 kt (7.5 ms^{-1}) is found within a shear feature and such feature overlaps with any of the ARENA (AREa Noted for Attention) boxes of the runway approach/departure corridors (see Figure 4), an alert with the wind shear magnitude and the location affected will be generated. It should be noted that following the TDWR convention, except for the RWY ARENA, the ARENA boxes at 1 NM, 2 NM and 3 NM from the runway ends are 1 NM x 1NM in size.

Figure 3 shows a display of the shear features identified by the RAGA prototype (from a 0.0-degree PPI scan) and the wind shear alerts generated for a wind shear event induced by sea-breeze. Around the time of the display, an aircraft reported wind shear of -15 kt / +35 kt at 100 ft (30 m) over the 07L approach corridor.

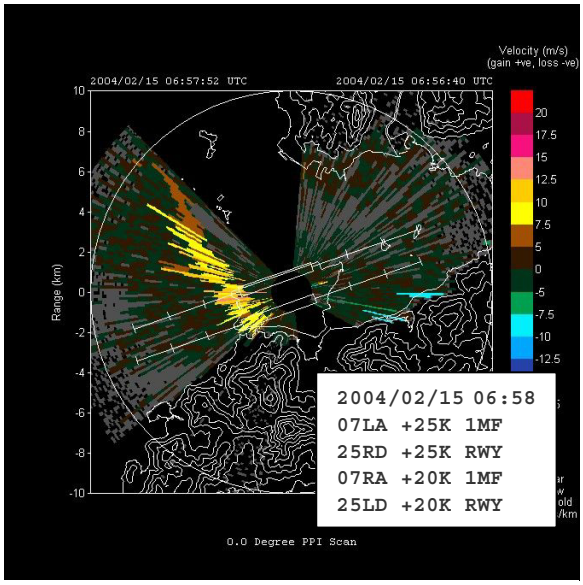

Figure 3. Display of the RAGA prototype. A 20-25 kt radial shear is detected along a sea breeze convergence line lying across the western corridors. Inset is the alphanumeric alerts generated by the algorithm.

3.2 Formulation and Performance

During initial formulation, the 0.0- and 1.0-degree PPI scans were used to generate alerts for all arrival corridors while the 4.5-degree PPI scans were used to generate alerts for all departure corridors.

The performance of RAGA was evaluated with reference to wind shear reports provided by aircraft landing at or departing from HKIA. The evaluation is

based on commonly used performance metrics including the probability of detection (POD), false alarm rate (FAR) and alert duration per hit (APH). Since "null' reports (i.e. headwind/tailwind change less than 15 kt) are not always available from aircraft, APH is used to supplement FAR to provide indications on whether or not alerts are excessive. The critical success index (CSI) could also be derived from the POD and FAR information. The algorithm has since been tuned to maximize POD while minimizing FAR and APH (hence maximizing CSI). Initial evaluation results indicate that while the POD of RAGA was high (over 90%), the FAR and APH were also on the high side. Improvements to the algorithm were therefore required.

3.3 Algorithm Enhancements

In-depth investigation suggested that the high FAR and APH were primarily due to the vertical separation between the PPI scans and the flight paths and that wind shear is often localized. For example, the laser beams of the 0.0-degree PPI scan align best with the arrival corridor only at about 1 NM from the runway ends. Therefore, by using the 0.0-degree PPI scan to generate alerts for the whole arrival corridor, the shear features detected on the PPI scan at the far end (e.g. at 3 NM) are located more than a hundred metres below the flight path. Shallow wind shear structures not affecting the flight path may therefore be captured by RAGA based on the 0.0-degree PPI scan, thus resulting in perceived false alarms to pilots, even though wind shear is present nearby. Similarly, quasi-stationary terrain-induced wind structures located near the Lantau terrain just to the south of the flight paths (around 1 km or less away) could also be captured by RAGA, leading again to perceived false alarms.

To address these issues, a Hazard Coverage Area (HCA) has been introduced for each PPI scan to refine wind shear detection by RAGA to within the HCA (see Figure 4). Since then, the performance of RAGA improves significantly with POD still over 90% while FAR and APH has reduced by half.

4. ALGORITHM II: GLIDE PATH SHEAR ALERT GENERATION ALGORITHM

4.1 Description of Algorithm

Another algorithm developed in parallel with RAGA is the GLIde path shear alert Generation Algorithm (GLYGA). In contrast to RAGA which is LIDAR-centric, GLYGA is designed with aircraft's perspective of wind shear (i.e. wind changes along the flight path) in mind.

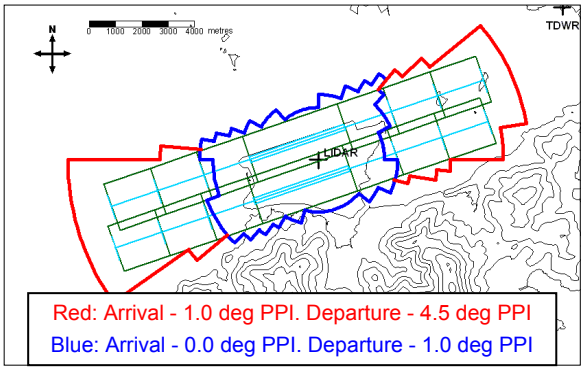

Figure 4. Diagram showing Hazard Coverage Area of PPIs at three different elevations angles, namely 0.0, 1.0 and 4.5 degrees. The ARENA boxes for the runways and approach/departure corridors are also indicated.

The algorithm starts with constructing headwind profiles along the flight paths. For each flight path, a headwind profile is constructed from Doppler velocities from LIDAR data points lying closest to it, i.e. within a horizontal distance of 1000 ft (300 m) and a vertical distance of 200 ft (60 m) (see Figure 2(b)). Wind shear features are detected from these profiles through a set of procedures adapted from studies of Woodfield and Woods (1983) and Woodfield (1994). In these studies, wind shear experienced by aircraft was identified from the headwind profile reconstructed from onboard flight data using the Peakspotter Program described by Jones and Haynes (1984). The significance of individual wind shear features identified from a headwind profile is considered based on the factor $\Delta V / L^{1/3}$, where ΔV = headwind/tailwind change and L = ramp length over which the wind speed change occurs. Wind shear features with ramp lengths between 400 m and 4000 m detected by GLYGA with ΔV in excess of a predefined threshold will trigger the generation of an alert for the corridor concerned (between 0 and 3 NM from the runway end). Information on the location, magnitude and the corridor being affected is given, based on the "First Encounter – Maximum Intensity" principle adopted for the TDWR (HKO and IFALPA, 2002).

Figure 5 shows the prototype GLYGA display for a terrain-induced wind shear event. The constructed

headwind profiles, detected wind shear features and alerts generated for the 8 runway corridors (4 for the 07 direction and 4 for the 25 direction) are shown together with the 2-dimensional Doppler velocity patterns on the 1.0-degree and 4.5-degree PPI scans. Within 5 minutes after the time of the display, an aircraft reported wind shear of -10 kt / +20 kt at 600 ft (180 m) over the 07L approach corridor.

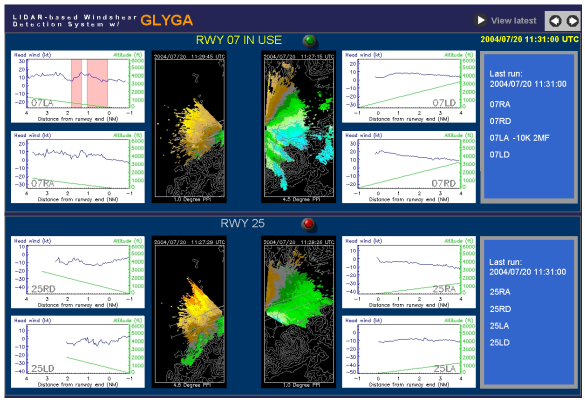

Figure 5. Display of the GLYGA prototype. The locations of detected wind shear along 07L approach corridor are shaded in red on the corresponding headwind profile (upper left). The corresponding alphanumeric alert is given in the boxes on the right.

4.2 Formulation and Performance

In the initial phase of algorithm development, data from the three PPI scans (at elevation angles of 0.0, 1.0 and 4.5 degrees) were used to construct the glide path headwind profiles. The threshold to trigger the generation of alert is user-adaptable to facilitate tuning in view of possible attenuation in the detected shear magnitude due to the angular separation between the LIDAR beams and the flight paths.

The results of the initial phase indicate that while GLYGA has somewhat lower POD compared with RAGA, its FAR and APH are significantly smaller, and hence better in this regard.

4.3 Algorithm Enhancements

Even though data from multiple PPI scans are used to create the headwind profile for each flight path, parts of the profile are nevertheless derived from data points at a distance from the flight path. Furthermore, detailed studies indicate that the constructed profiles may sometimes contain artificial discontinuities where adjacent points are selected from PPI scans at different elevation angles, especially when shallow wind shear structures are present.

In view of the discussion under Section 3.3, the difficulty of obtaining representative headwind profiles along the flight paths is apparently common to both RAGA and GLYGA. To address this issue, new Glide Path (GP) scans were recently introduced. In contrast to the commonly used PPI and RHI scans which provide data at constant elevation and azimuthal angles respectively, GP scans are performed to provide data along and in the vicinity of the flight paths. This is achieved by programming the LIDAR scanner to scan as close to the flight paths as possible based on a sequence of user-defined elevation and azimuthal angles (see Figure 6). The current scan strategy allows re-visit time of about 2 minutes for GP scans towards the most frequently used glide paths. A number of PPI and RHI scans with re-visit time of around 4 minutes are retained for operational wind shear monitoring by forecasters.

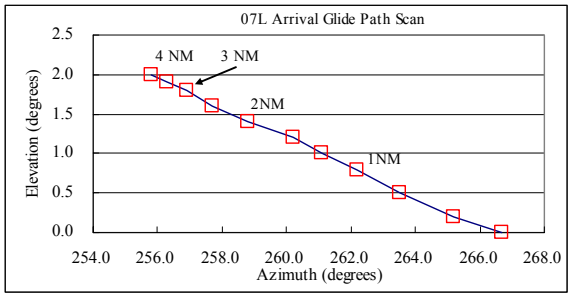

Figure 6. An example showing the elevation and azimuthal angles for the LIDAR scanner to scan along the 07L approach corridor.

Experience so far indicates that GLYGA performs better based on the new GP scans, especially for terrain-induced events which can be of rather small scale and localized. On-going tuning of the algorithm is being conducted to reduce false alarms arising from Doppler velocity spikes which occasionally appear on the constructed headwind profiles and to optimize the overall performance of GLYGA with regard to pilot wind shear reports.

5. CONCLUSION

Two different approaches to automatically generate wind shear alerts based on LIDAR Doppler velocity data are described. Neither one of them excels in all aspects. RAGA has a 2-dimensional

perspective and is able to generate wind shear alerts whenever significant radial shear is detected within the HCA. It works best in detecting wind shear caused by shear lines, e.g. sea breeze fronts and gust fronts, crossing the approach/departure corridors. On the other hand, GLYGA is capable of detecting wind shear along the flight paths, especially after GP scans were introduced. The GP scans are able to pick up localized wind structures impacting on the flight paths which cannot otherwise be captured by conventional PPI scans. However, its 1-dimensional perspective along the glide paths makes it difficult to detect nearby features which may move in sideway and affect the glide paths between consecutive scans. This is especially challenging for terrain-induced events which can be transient and sporadic in nature (HKO and IFALPA, 2002).

The RAGA and GLYGA prototypes are currently running round the clock to collect more data for detailed performance verification. In addition to pilot reports, on-board flight data will also be used in the verification. On-going research is being conducted to refine the algorithms and to develop an integrated system with advantages of both algorithms.

6. REFERENCES

Hong Kong Observatory (HKO) and International Federation of Air Line Pilots' Associations (IFALPA), 2002: *Windshear and Turbulence in Hong Kong – information for pilots*, 24 pp.

International Electrotechnical Commission (IEC), 2001: *Safety of laser products – Part 1: Equipment classification, requirements and user's guide.* IEC 60825-1 Edition 1.2, 115 pp.

Jones, J.G. and A. Haynes, 1984: A Peakspotter Program Applied to the Analysis of Increments in Turbulence Velocity. *RAE Technical Report 84071.*

Merritt, M.W., D. Klingle-Wilson and S.D. Campbell, 1989: Wind shear Detection with Pencil-Beam Radars, *The Lincoln Laboratory Journal, Volume 2, Number 3.*

Shun, C.M., C.M. Cheng, and O. Lee, 2003, "LIDAR Observations of Terrain-induced Flow and its Application in Airport Wind Shear Monitoring", *International Conference on Alpine Meteorology (ICAM) and Mesoscale Alpine Programme (MAP) Meeting, Brig, Switzerland, 19-23 May 2003*.

Shun, C.M. and S.Y. Lau, 2002: Implementation of a Doppler LIght Detection And Ranging (LIDAR) system for the Hong Kong International Airport, *Preprints, 10th AMS Conf. on Aviation, Range and Aerospace Meteorology*, 255-256.

Shun, C.M., S.Y. Lau, C.M. Cheng, O.S.M. Lee, and H.Y. Chiu, 2004: LIDAR Observations of Wind Shear Induced by Mountain Lee Waves, *11th Conference on Mountain Meteorology and MAP Meeting 2004*.

Woodfield, A.A., 1994: Wind Shear and its effects on aircraft. *AGARD Lecture Series on 'Flight in an Adverse Environment', AGARD LS-197.*

Woodfield, A.A. and J.F. Woods, 1983: Worldwide Experience of Wind Shear During 1981-1982. *AGARD Flight Mechanics Panel Conference on 'Flight Mechanics and system design lessons from Operational Experience', AGARD CP No. 347.*